MITOTIC PHASE BASED DETECTION OF CHROMOSOME SEGREGATION ERRORS IN EMBRYONIC STEM CELLS

A. El-Labban [1*] *C. Arteta* [1] *A. Zisserman* [1] *A. W. Bird* [2] *A. Hyman* [3]

[1]Department of Engineering Science, University of Oxford, United Kingdom
[2]Max Planck Institute for Molecular Physiology, Dortmund, Germany
[3]Max Planck Institute of Molecular Cell Biology and Genetics, Dresden, Germany

ABSTRACT

The detection of chromosome segregation errors in mitosis is an important area of biological research. Due to the rarity and subtle nature of such errors in untreated cell lines, there is a need for automated, high-throughput systems for quantifying the rates at which such defects occur.

This paper presents a novel approach to detecting subtle chromosome segregation errors in mitosis in embryonic stem cells, targeting two cases: misaligned chromosomes in a metaphase cell, and lagging chromosomes between anaphase cells.

Our method builds on existing approaches for analysis of other cell lines (e.g. HeLa) which label mitotic phases through mitosis and detect substantial deviations from normal mitotic progression. We apply these to more challenging, denser, stem cell lines. Leveraging the mitotic phase labelling allows us to detect smaller, more subtle defects within mitosis. This results in a very high recall rate, as necessary for detection of such rare events.

1. INTRODUCTION

When a cell divides, it must segregate all of its chromosomes equally into two daughter cells. Errors in chromosome segregation can lead to the gain or loss of chromosomes in a cell, resulting in a state known as aneuploidy. Aneuploidy can lead to problems in development, and cancer cells frequently display aneuploidy resulting from a high rate of chromosome missegregation, a condition termed chromosomal instability [1].

Compared to many cancer cell lines routinely studied, such as HeLa (human epithelial adenocarcinoma) cells, embryonic stem cells have relatively low levels of chromosome instability [2], making them useful for identifying conditions that lead to small but biologically significant increases in chromosome segregation defects. It is also important to be able to determine accurately the degree of chromosome segregation errors and aneuploidy in stem cell lines, as they become candidates for medical treatments.

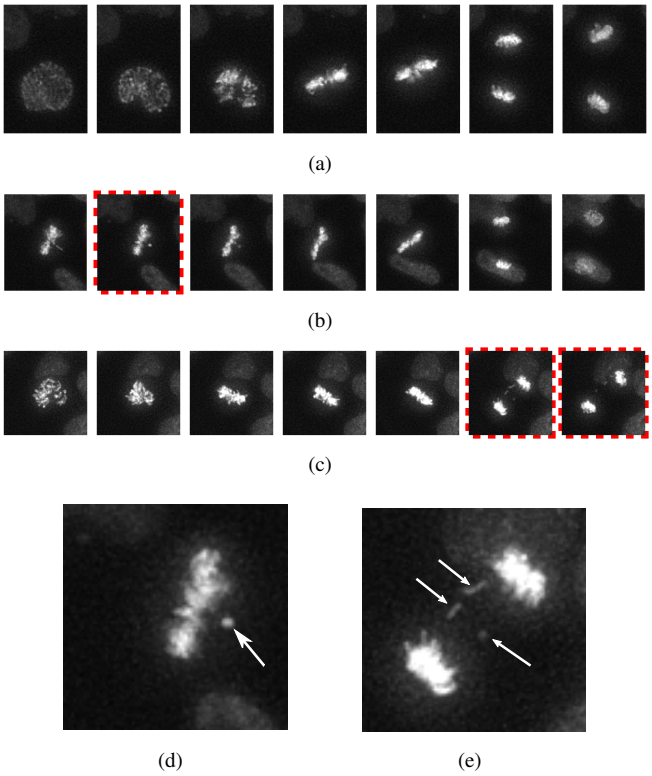

Fig. 1. **Examples of chromosome segregation defects.** (a) Track of cell undergoing mitosis normally. (b) & (c) Tracks of two cells undergoing mitosis, frames with errors are highlighted in red (dashed). (d) & (e) Enlarged view of frames with defects, indicated with white arrows. (b) & (d) Misaligned chromosome, fails to align to metaphase plate during mitosis. (c) & (e) Lagging chromosomes, not segregated into either daughter cell during mitosis.

Due to the rarity of such errors in stem cell lines, large amounts of data need to be analysed to detect statistically significant changes in error frequency under different experimental conditions. Additionally, due to the subtlety of the defects, human annotation can be difficult and time-consuming. There is therefore a need for automated high-throughput

*This work was supported by ERC grant VisRec no. 228180 and the RCUK Centre for Doctoral Training in Healthcare Innovation (EP/G036861/1).

methods for quantifying this data.

There has been substantial recent work on automated image analysis in sequences of mitotic cells, predominantly focusing on HeLa cells [3, 4, 5, 6]. These approaches either detect perturbations in mitosis based on durations of mitotic phases [3, 4], or as morphologies which differ substantially from those observed in normal mitotic progression [3, 5] e.g. binuclear or polylobed cells. All prior work uses a common overall processing pipeline: frames are first segmented into individual cells using image processing operations such as adaptive thresholding and watershed algorithms [3, 4, 5], or a combination of a linear classifier and graph cuts [6], and the cells are then tracked throughout the sequence. Next, frames are classified into mitotic phases or a more extensive set of morphologies, either using a support vector machine followed by temporal correction [3, 4, 5], or by directly using temporal models [6].

The novel aspect of this work is that it aims to detect much more subtle mitotic errors than previous methods, which focused on detection of substantial variations from normal mitoses (i.e. durations or morphologies). Our method leverages mitotic track phase labelling information to significantly reduce the search space for defects to just the phases in which the desired defects are expected to occur. This approach uses existing methods to detect and track mitotic cells and label the mitotic phases over time, though applied to a different cell type than previous methods – embryonic stem cells rather than HeLa cells. The detection of errors targets two cases: either around a metaphase cell for misaligned chromosomes or between anaphase cells for lagging chromosomes, as illustrated in Figure 1. This 'phase aware search' results in reliable detections, with a high recall rate, as required for this application given the rarity of defects.

2. DATA

The data consists of 40 sequences of mouse embryonic stem cells expressing fluorescent histone-GFP protein to visualize chromosomes. Images were acquired on a widefield fluorescence microscope with a $40\times$ objective. Cells were imaged every 4 or 5 minutes, and for each time point a z-stack of 5 images at 2.5 micron spacing was acquired. Final image sequences were then deconvolved and z-stacks projected. The resolution is 480×480 pixels. Sequences initially contain 19 cells on average, approximately 760 in all sequences, a number which increases as cells divide or new ones move into focus, and last for an average duration of 170 frames. In total, over all frames in all sequences, there are approximately 13×10^4 possible individual cell detections. Sequences contain from 2 up to 41 mitoses. In total, 62% of all cells in the dataset undergo mitosis, giving 473 mitoses, of which 10 contain a misaligned chromosome error and 10 contain a lagging chromosome error (slightly over 4% of the 473 mitoses are defective). Mitoses typically last 10-12 frames, and defects are visible for at most 3 frames in mitotic tracks i.e. fewer than 0.2% of all possible individual cell detections are mitoic and 0.03% contain chromosome segregation errors.

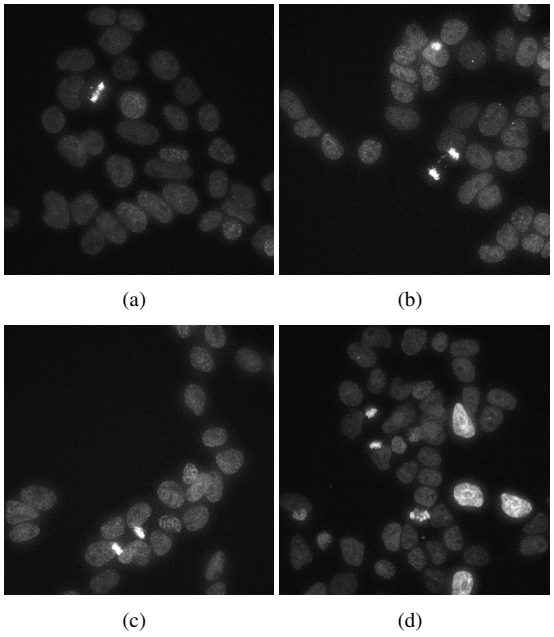

Fig. 2. **Four typical frames from the data.** There is one visible mitosis in each frame. The challenges of this dataset include densely clustered cells, overlap of mitotic and interphase cells (e.g. in (b)-(c)), artifacts from dead cells (e.g. top of (b) and middle of (d)), and significant variations in interphase cell brightness (e.g. the four interphase cells on the right of (d)).

The data presents a number of challenges, illustrated in Figure 2, including densely clustered cells, overlap of mitotic and interphase cells, artifacts from dead cells, and significant variations in interphase cell brightness. The chromosomes that must be detected are extremely small: either blobs only 2-3 pixels in diameter, or as slightly elongated, strand-like objects 4-5 pixels long and 1-2 pixels wide.

3. METHOD

We follow a three stage approach for detecting chromosome segregation defects: first detecting and tracking mitotic cells, second labelling the phase of mitosis in every frame of the tracks, and finally detecting defects in metaphase (misaligned chromosomes) and anaphase (lagging chromosomes).

3.1. Detection & Tracking

Due to the very high density of cells in the data, resulting in a large proportion of cells touching or overlapping, detecting and tracking all cells in a sequence would be an extremely challenging task; simple foreground segmentation techniques would not differentiate between cells. Also, it is unnecessary to detect and track all cells when the purpose is detecting defects in mitosis. Instead, we detect only mitotic cells (prometaphase, metaphase, anaphase and telophase) which can be distinguished from interphase cells as they are typi-

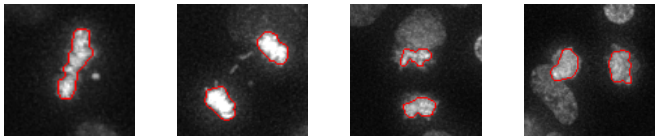

(a) (b) (c) (d)

Fig. 3. **Example detection results.** Detected extremal region boundaries overlaid on images. Detection gives good segmentation boundaries and copes with overlapping or touching cells e.g. in (c) and (d). View in colour to see overlaid boundaries.

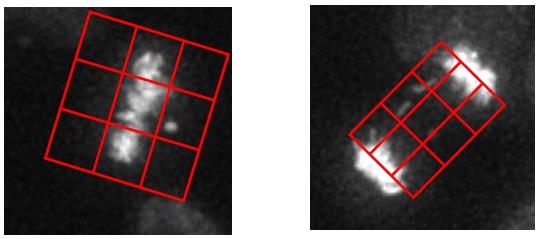

(a) (b)

Fig. 4. **Aligned regions of interest for defect detection.** (a) Misaligned chromosomes occur along the major axis of metaphase cells. (b) Lagging chromosomes appear between anaphase cells. Detections within these regions are encoded in a 3×3 bin spatial histogram. Segmented cell regions, shown in Figure 3, are excluded from the region of interest.

cally substantially brighter in appearance. The extremal region based approach of [7] is used for this purpose. This method involves first proposing hundreds of candidate extremal regions, and then selecting the regions of interest using a classifier together with a non-overlap constraint. It can robustly detect mitotic cells even when they overlap with interphase cells, as can be seen in Figure 3, and the resulting regions provide good chromatin segmentations for use in subsequent steps. For brevity, the chromatin segmentations will be referred to as cells in the remaining sections.

Cells are then associated from frame to frame by a nearest neighbour approach using a feature consisting of centroid position and size, and incorporating validation gating in the form of an association threshold. This approach is sufficient to cope with the relatively well spaced out detections, both spatially and temporally.

A post-processing stage is applied to remove false positive tracks: a linear classifier is used to remove tracks of artifacts from cell death, and non-mitotic cells which are bright enough to be detected. The features used for this consist of the mean, standard deviation, maximum and minimum values of cell brightness and size over a track. These features should vary substantially as a cell undergoes mitosis but remain reasonably constant for artifacts and interphase cells.

3.2. Phase labelling

For phase labelling we adopt the approach of [6]. As the performance of this method improves when a track is sufficiently long to contain all mitotic phases, the detected mitotic tracks are continued three frames forward and backwards in time to obtain some frames with the cells in interphase, allowing for better normalisation of the features.

3.3. Defect detection

For detection of the defective chromosomes, a two stage approach is used: first, candidate structures are detected in a region of interest around the cell, and second detections are filtered based on a number of intensity and spatial characteristics. The region of interest is defined where defects are expected to occur – orthogonal to the major axis of metaphase cells, or between dividing anaphase cells. Example regions are illustrated in Figure 4.

Within the interest regions, candidate misaligned/lagging chromosomes are initially detected as blobs as local maxima of Lapacian of Gaussians filter response. The filtering operation is carried out at two different scales ($\sigma = 1, 2$ pixels) to account for variation in defect sizes. Note, the chromatin segmented region determined in Section 3.1 is excluded when proposing candidates and in other subsequent processing.

The candidates contain a large number of false positives primarily due to interference from other nearby cells. The purpose of the second stage is a filter to remove these false positives.

For the intensity based filtering step, we observe that actual mitotic defect detections have pixel intensities closer to the chromatin in the segmented cell than the background portion of the interest region. Therefore, we assume that the probability of a blob corresponding to a mitotic defect is proportional to the ratio of intensity differences:

$$p(defect|i_{blob}) \propto \exp\left(\frac{-(i_{blob} - i_{cell})^2}{2\sigma_{cell}^2} - \frac{-(i_{blob} - i_{bg})^2}{2\sigma_{bg}^2}\right)$$

where i_{blob} is the pixel intensity at the blob detection, i_{cell} and σ_{cell} are the mean and standard deviation of chromatin pixel intensities within the segmented cell, and i_{bg} and σ_{bg} are the mean and standard deviation of pixel intensities in the interest region background. A threshold, τ, on this measure removes false positives. The image is then thresholded based on intensity at each detection, with the resulting segmentation used to estimate the size of the detected blob. Segmentations larger than individual chromosomes are discarded.

The remaining detections are then encoded in a 3×3 bin spatial histogram. Histogram bin counts are weighted by the magnitude of detected peaks in the filter response, reducing the contribution of any remaining peaks caused by image noise. Entropy is then used as a measure to define defects, based on the observation that true defects will appear as well localised detections, and consequently generate histograms with low entropy.

4. RESULTS

Results are reported in Table 1 for the cell detection and mitotic defect detection components of this work. For each of

	True Pos.	False Pos.	False Neg.	True Neg.	Precision	Recall
Mitosis detection (frame)	2853	2658	852	$\approx 13 \times 10^4$	0.52	0.77
Mitosis detection (track)	409	19	64	≈ 750	0.96	0.86
Defect detection (frame)	23	80	12	4491	0.22	0.66
Defect detection (track)	18	47	2	364	0.29	0.90

Table 1. Results for the two key stages of the method – mitotic cell detection, and defect detections. The performance of each stage is assessed on a frame-by-frame basis and on a whole track basis. Mitotic defect detection results are based on detected mitotic tracks from the previous stage. The true negative values for mitosis detection are estimates, as ground truth data is unavailable for non-mitotic cells and tracks.

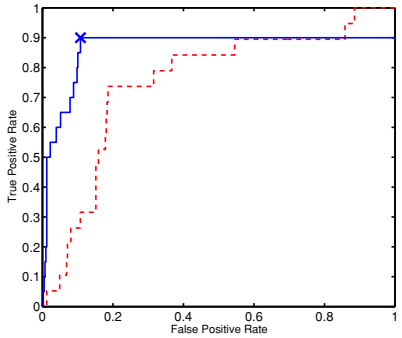

Fig. 5. **ROC curve of defective mitotic track detection.** The red (dashed) curve uses only candidate defects (before filtering) as described in the first stage of Section 3.3. The blue curve incorporates mitotic phase and spatial information filters. The operating point used for results in Table 1 is indicated with a blue '$\times$'.

these, performance values are given for two conditions: individual frame detections and whole track detections. The track performance is particularly important since detecting a defective mitotic track is still useful for analysing large scale biological data even if one or two frames containing defects are missed.

For the mitotic cell detection part of this work, the 40 sequences in the dataset are divided into two equal partitions of 20 for training and testing. Within the training partition, two-fold cross-validation is used to set parameters of the detection system. Training is then carried out on the full 20 sequence partition and tested on the remaining half of the data. The partitions are then switched and the training and testing process is repeated to obtain mitotic cell detections for all 40 sequences. This results in very high detection accuracies, with overall precision and recall values of 0.96 and 0.86 for mitotic track detection. False positive track detections are mostly caused by artifacts remaining from cell death and oversegmentations of correctly detected cells.

The defect detection results are based only on detected mitotic tracks from the first stage. All of the 20 mitotic tracks in the dataset containing defects are detected. For the mitotic defect detection, the threshold, τ, described in Section 3.3 is varied to produce ROC curves, as shown in Figure 5. This results in a very high rate of recall, with only two tracks with defects missed. Precision is lower due to the significant imbalance in the data. The two false negative tracks which occur are both lagging chromosomes in anaphase cells. All misaligned chromosomes in metaphase are correctly detected.

5. CONCLUSION

We have presented a novel method for detecting very rare and subtle mitotic errors in large volumes of microscopy images. Our method is useful as a filter for further biological analysis, as it reduces the amount of data to be analysed manually by several orders of magnitude, although further work can improve the precision. With the availability of more data additional types of mitotic errors may be detected, or the two addressed here may be further sub-categorized. Additionally, classifiers could be trained to further improve precision.

6. REFERENCES

[1] D. A. Compton, "Mechanisms of aneuploidy," *Current Opinion in Cell Biology*, 2011.

[2] S. Saito, K. Morita, A. Kohara, T. Masui, M. Sasao, H. Ohgushi, and T. Hirano, "Use of BAC array CGH for evaluation of chromosomal stability of clinically used human mesenchymal stem cells and of cancer cell lines," *Human Cell*, 2011.

[3] N. Harder, F. Mora-Bermúdez, W. J. Godinez, A. Wünsche, R. Eils, J. Ellenberg, and K. Rohr, "Automatic analysis of dividing cells in live cell movies to detect mitotic delays and correlate phenotypes in time.," *Genome research*, 2009.

[4] M. Held, M. H. A. Schmitz, B. Fischer, T. Walter, B. Neumann, M. H. Olma, M. Peter, J. Ellenberg, and D. W. Gerlich, "CellCognition: time-resolved phenotype annotation in high-throughput live cell imaging.," *Nature methods*, Aug 2010.

[5] B. Neumann, T. Walter, J.-K. Hériché, J. Bulkescher, H. Erfle, C. Conrad, P. Rogers, I. Poser, M. Held, U. Liebel, C. Cetin, F. Sieckmann, G. Pau, R. Kabbe, A. Wünsche, V. Satagopam, M. H. A. Schmitz, C. Chapuis, D. W. Gerlich, R. Schneider, R. Eils, W. Huber, J.-M. Peters, A. A. Hyman, R. Durbin, R. Pepperkok, and J. Ellenberg, "Phenotypic profiling of the human genome by time-lapse microscopy reveals cell division genes," *Nature*, vol. 464, no. 7289, pp. 721–727, Apr 2010.

[6] A. El-Labban, A. Zisserman, Y. Toyoda, A. W. Bird, and A. Hyman, "Dynamic time warping for automated cell cycle labelling," in *MIAAB*, 2011.

[7] C. Arteta, V. Lempitsky, J. A. Noble, and A. Zisserman, "Learning to detect cells using non-overlapping extremal regions," in *MICCAI*, 2012.